



Discover Generics

Cost-Effective CT & MRI Contrast Agents



FRESENIUS
KABI

WATCH VIDEO

AJNR

Volumetric Perfusion CT Using Prototype 256-Detector Row CT Scanner: Preliminary Study with Healthy Porcine Model

Shinichiro Mori, Takayuki Obata, Naoshi Nakajima,
Nobutsune Ichihara and Masahiro Endo

This information is current as
of June 25, 2025.

AJNR Am J Neuroradiol 2005, 26 (10) 2536-2541
<http://www.ajnr.org/content/26/10/2536>

Volumetric Perfusion CT Using Prototype 256–Detector Row CT Scanner: Preliminary Study with Healthy Porcine Model[□]

Shinichiro Mori, Takayuki Obata, Naoshi Nakajima, Nobutsune Ichihara, and Masahiro Endo

Summary: This is a preliminary demonstration of volumetric perfusion CT of the brain in domestic pigs by using a prototype 256-detector row CT. Scan range is approximately 100 mm in the craniocaudal direction with 0.5-mm section thickness. The 256–detector row CT is an easily available imaging technique that can provide volumetric cine imaging, CT angiography, and perfusion CT in a wide craniocaudal coverage simultaneously.

A number of methods for the evaluation of acute stroke and brain ischemia have been introduced, including xenon-enhanced CT, positron-emission tomography (PET), single-photon emission CT (SPECT), and MR imaging. These methods, however, are not widely available outside large hospitals. In contrast, the equipment required for dynamic CT perfusion in cerebral perfusion imaging is generally available in most hospitals. The major clinical applications of perfusion CT are in stroke and oncology, including nephrologic and hepatologic oncology. The organ of interest is scanned in cine mode, with the table kept stationary while the contrast medium is injected into the patient and distributed via the circulation. Various image analysis algorithms have been developed during the past 2 decades, and clinical utility has been expanded to include the measurement of cerebral blood flow (CBF), cerebral blood volume (CBV), and mean transit time (MTT) (1).

A principal limitation of CT perfusion by using conventional CT, including multidetector CT (MDCT), however, is its limited sample volume. The latest MDCT now incorporates 64 segments with a segment size of 0.5–0.625 mm at the center of rotation, which represents a substantial improvement from conventional MDCT, especially in cardiac imaging. The maximum axial field of view is <40 mm, however, which makes the location of investigation critical, because

only a limited section of the organ of interest can be examined. Although identification of the pathologic area by helical scanning before perfusion CT remains possible, the use of MDCT may result in erroneous perfusion CT mapping of the pathologic area or incomplete coverage of the whole pathologic area.

To increase the coverage of perfusion CT studies in the craniocaudal direction (volumetric perfusion CT), we developed a prototype 256–detector row CT (2). This increase in the number of detector rows allows an isotropic resolution of less <0.5 mm and wide craniocaudal coverage (approximate length 100 mm) in a single rotation. The 256–detector row CT thereby promises to increase the amount of diagnostic information obtainable and solve some of the limitations of present helical CT methods in cardiovascular circulation (3), kinematics, and radiation therapy planning for image-guided radiation therapy (IGRT) and 4D radiation therapy.

Here we describe a preliminary investigation of volumetric perfusion CT by using the 256–detector row CT in the evaluation of 2 healthy domestic pigs.

Materials and Methods

Prototype 256–Detector Row CT

The prototype 256–detector row CT (2, 4) uses a wide-area cylindrical 2D detector designed on the basis of present CT technology and mounted on the gantry frame of a 16–detector row CT (5; Aquilion, Toshiba Medical Systems, Otawara, Japan). It has 912 (transverse) \times 256 (craniocaudal) elements, each approximately 0.5 mm \times 0.5 mm at the center of rotation. In designing this prototype, we favored wide radiographic coverage in the craniocaudal axis, which required tilting the radiograph tube a few degrees. This approach had several disadvantages, including heavy coriolis forces on the tube's bearing due to angular momentum conservation, which necessitated that the rotation time of the gantry be restricted to 1.0 second to protect the bearing. The 128-mm total beam width allows the continuous use of several collimation sets (eg, 256 \times 0.5 mm, 128 \times 1.0 mm, 64 \times 2.0 mm). Craniocaudal coverage of the 256–detector row CT is approximately 100 mm per rotation. Data sampling rate is 900 views per rotation, and dynamic range of the analogue-digital converter is 16 bits. The detector element consists of a Gd₂O₂S ceramic scintillator and single-crystal silicon photodiode, as used for MDCT.

Reconstruction is done with a Feldkamp-Davis-Kress algorithm (6). Reconstruction of a 512 \times 512 \times 256-voxel data set by a high-speed image processor in a field programmable gate array-based architecture took <1 second.

Received February 26, 2005; accepted after revision May 13.

From the Departments of Medical Physics (S.M., M.E.) and Medical Imaging (T.O.), National Institute of Radiological Sciences, Chiba, Japan; Shimodate Animal Hospital (N.N.), Ibaraki, Japan; and Laboratory of Anatomy, School of Veterinary Medicine (N.I.), Azabu University, Kanagawa, Japan.

Address correspondence to Shinichiro Mori, MS, 4-9-1 Anagawa, Inage-ku, Chiba-shi, Chiba, 263-8555, Japan.

[□]The online version of this article contains supplemental videos at <http://www.ajnr.org>.

Data Processing

The theoretical basis for volumetric perfusion CT analysis is the use of CBF, CBV, and MTT for deconvolution analysis. This analysis assumes that the contrast medium is not diffusible, because nondiffusibility is a reasonable assumption in the brain. Here the tissue concentration function $C_t(t)$ was calculated as follows:

$$C_t(t) = F \cdot C_a(t) \otimes R(t),$$

where \otimes is the convolution operator, F is cerebral blood flow, $C_a(t)$ is the measured arterial concentration of contrast media, and $R(t)$ is the time enhancement curve of the tissue obtained by the contrast-injected cine scan. The cine scanning measured $C_t(t)$ and $C_a(t)$ and generated deconvolution between them. CBF and CBV were then calculated from $F R(t)$. MTT can be calculated by the central volume principle (7) as follows:

$$MTT = \frac{CBV}{CBF}.$$

CBF, CBV, and MTT maps were generated by using modified commercial deconvolution-based software (CT Perfusion, Toshiba Medical Systems) for volumetric perfusion CT analysis. The analyses were generated by simply extending the conventional 2D analysis (pixel-based) to a 3D analysis (voxel-based). This analysis was used to create time-enhancement curves for each voxel, which were linearly related to the time attenuation curves (TDCs) for the first pass of an iodinated contrast material. Small round regions of interest measuring 4–8 mm² were placed manually by a trained research assistant onto the anterior cerebral artery and the superior sagittal sinus to provide arterial and venous TDCs, respectively.

Image quality and accuracy of the perfusion map were evaluated by a board-certified radiologist and 2 veterinarians, each of whom had >10 years of clinical experience. Image quality was assessed by reference to experience-based standards. Reading of the images in multiple planes took about 30 minutes.

Technique for Volumetric Perfusion CT Imaging

All animal procedures were approved by the National Institute of Radiologic Sciences' institutional review board. Two domestic pigs weighing 25 kg were mechanically ventilated under isoflurane anesthesia, and an introducer was positioned in the inferior vena cava via the external carotid artery.

After an initial scout topogram of the head was made, injection of 50 mL of nonionic iodinated contrast material (Iopamiron 370; Nihon Schering, Osaka, Japan) was begun by using a power injector at a flow rate of 9.9 mL/s, followed by scanning in the cine mode with the gantry centered over the head. A 1-second delay between the start of administration and scanning was used, with scan parameters 120 kV, 200 mA, and 128 × 1.0 mm beam collimation. Because continuous scan time was limited by disk storage capacity, 1-second rotation time and 50-second total scan times were selected. Effective dose was 63.0 mSv/50 seconds. The volume elements (voxels) were 0.47 × 0.47 × 0.47 mm in a 512 × 512 × 216 data matrix covering a 240 × 240 × 102 mm volume with a 0.3-second time interval.

Results

The vascular system of a pig brain with and without cranial bones is shown in Figs 1A and 1B, respectively. Results showed contrast enhancement with 3D volume rendering after the start of injection (pig 1, Fig 1). The carotid arteries were best visualized on images obtained at approximately 5–10 seconds (Fig 1C), whereas enhancement of the sagittal venous sinus and infraorbital artery increased gradually from 8

to 16 seconds (Figs 1D and 1E). Enhancement of the lingual artery was decreased at 25 seconds (Fig 1F).

The nonenhanced sagittal section image shows fine structure at the start (0 seconds) of injection (Fig 2A). CT angiographs (CTAs; Fig 2B) obtained by subtracting nonenhanced images (Fig 2A) from the volumetric cine data show contrast enhancement at 14 seconds. Volumetric perfusion analyses for CBF, CBV, and MTT for pig 1 are shown in Fig 2C–E. Volumetric perfusion CT maps are superimposed on the sagittal image. In addition to the brain, the lingual arteries are also mapped.

The results of volumetric perfusion CT in an oblique plane at a 40° angle to the horizontal for pig 2 are shown in Fig 3. The CTA (Fig 3C) shows contrast enhancement 15 seconds after the start of contrast injection. Volumetric perfusion CT was done in the oblique plane with a maximum intensity projection (MIP) slab thickness of 6.0 mm and MIP slab position and angle parallel to the orbitomeatal line.

Volumetric perfusion CT results were optimized by fixing the position of the pig's head by using the patient belt and the wide coverage of the 256-detector row CT. The thin section thickness (1 mm) facilitated observation of anatomic sites.

Discussion

This study demonstrates a number of advantages of the 256-detector row CT compared with existing systems in terms of both the speed of data acquisition and volume of data provided.

First, the 256-detector row CT was designed to allow cine imaging over a craniocaudal distance of approximately 100 mm with a thin section thickness. The thin section cine image volume data can also be used to create cine loops, CT angiography, and perfusion maps on multiple planes. This is not possible with existing MDCT.

Second, any movement of the patient during repeated MDCT imaging of the same tissue volume for extended periods of time will result in perfusion value errors. Patient motion out of the image plane leads to data loss, though limited tracking of moving tissue from section to section in multisection studies may be possible. Because of its wider imaging area, however, the 256-detector row CT solves this sample volume limitation. This characteristic is of particular importance when the speed of clinical decision making is important, such as in emergency settings in acute stroke, brain ischemia, and intracranial hemorrhage.

Moreover, conventional interventional radiology by using fluoroscopy and CT fluoroscopy to guide interventional procedures constrains radiologists to understanding the relationship between catheter and vascular positions from 2D images alone, with limited information on depth direction. The 256-detector row CT overcomes this problem by providing volumetric cine images during interventional procedures, facilitating interventions and shortening examination times. Although spatial resolution of the 256-detector row CT

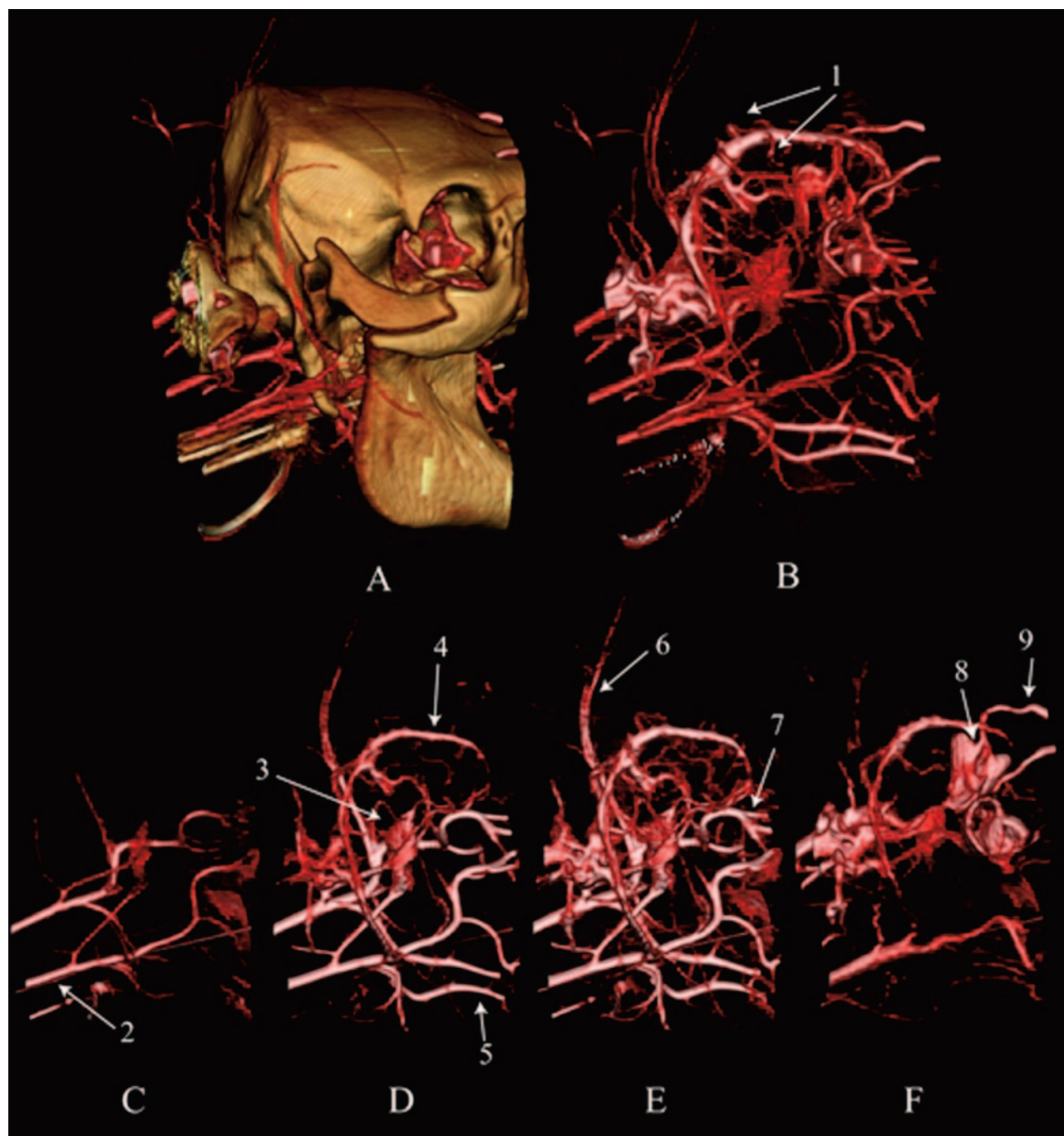


FIG 1. 3D volume rendering beginning 15 seconds after the start of injection (A) with and (B) without cranial bones. C, Shown 7 seconds after the start of injection. D, Slightly enhanced visualization of the superior sagittal sinus and inferior sagittal sinus (arrow) increasing gradually from 12 seconds after the start of injection. E, Optimum visualization of the superior sagittal sinus and inferior sagittal sinus 16 seconds after the start of injection. F, Decrease in enhancement of the superior sagittal sinus at 25 seconds after the start of injection. 1, dorsal cerebral veins; 2, carotid artery; 3, transverse facial artery; 4, sagittal venous sinus; 5, lingual artery; 6, caudal auricular artery; 7, infraorbital artery; 8, ophthalmic venous sinus; 9, supraorbital vein.

remains less than that of intra-arterial catheter examination, it is nevertheless a powerful noninvasive method allowing observation of the clear 3D angiogram in multiple planes continuously (Fig 1).

Further, in addition to the head, the 256-detector row CT may also be useful in perfusion studies of the chest and abdominal regions such as the liver and lung. Although voluntary or imposed breath-holding

techniques have been proposed to reduce or eliminate the effects of breathing motion during both CT imaging and perfusion studies, many patients cannot tolerate holding their breath. Respiratory gated volumetric perfusion CT may therefore improve examination comfort and reduce misregistration in calculating perfusion maps. Adoption to cardiac gated volumetric perfusion CT should also be feasible.

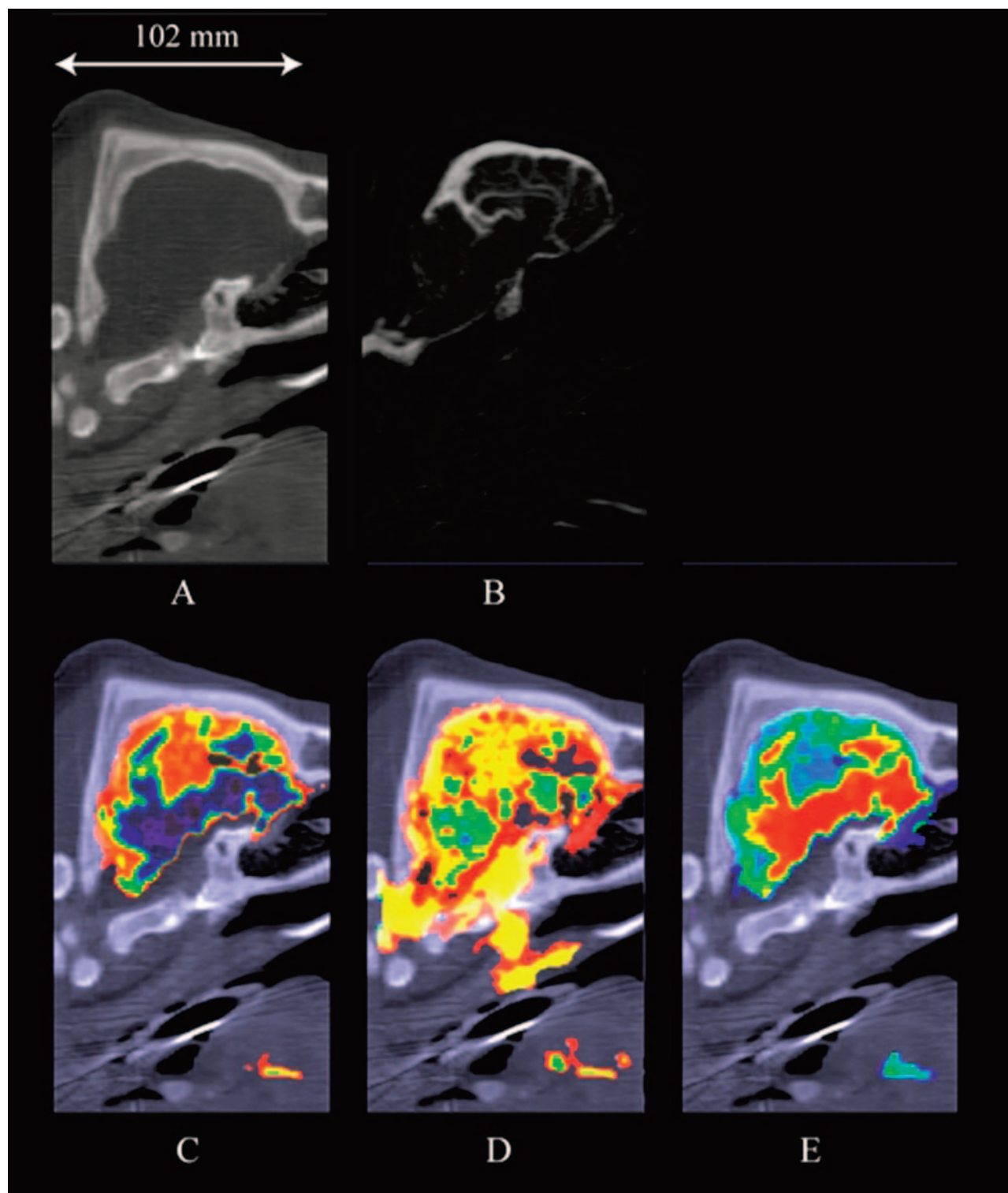


FIG 2. Results for a healthy domestic pig (pig 1). *A*, Nonenhanced sagittal image with a 6-mm section thickness. *B*, CTA in the sagittal plane at 14 seconds after the start of contrast injection. Various color ramps, selected according to user preference, were used to display the sagittal perfusion CT maps of (*C*) CBF, (*D*) CBV, and (*E*) MTT. These perfusion CT maps show enhancement of the lingual artery and vein in addition to the brain.

With regard to contrast media, CT examination requiring contrast medium is generally performed before CT perfusion scanning by helical scanning with a beam collimation of 1.0- or 1.5-mm thickness. This necessitates the administration of more than one con-

trast medium in the individual patient. In contrast, the 256-detector row CT acquires perfusion CT, CTA, and volumetric cine data simultaneously, thereby minimizing contrast medium dosage, as well as examination and equipment costs.

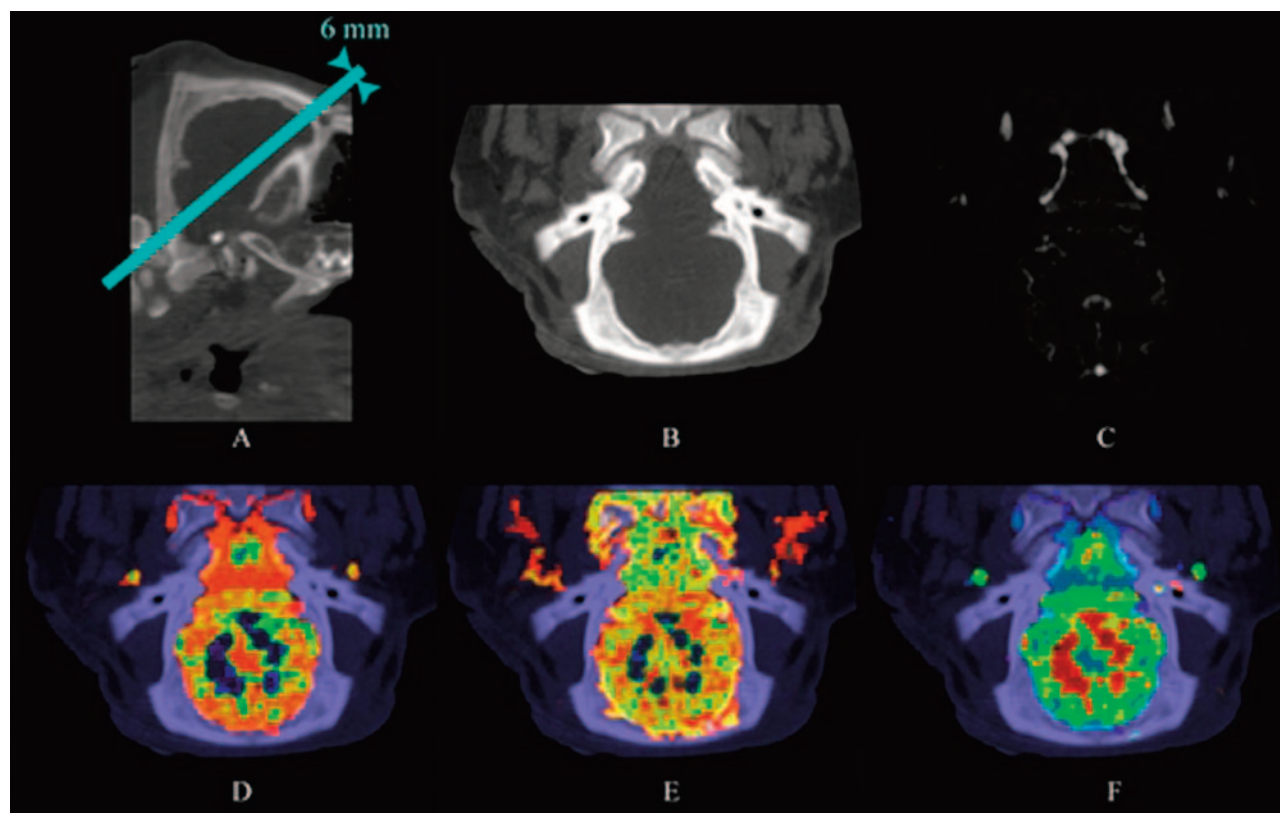


FIG 3. Results for a healthy domestic pig (pig 2). *A*, Nonenhanced sagittal image with a 6-mm section thickness. *B*, Oblique image at a 40° angle to the horizontal line shown in Fig 2*A*. *C*, CTA in an oblique plane at 14 seconds after the start of contrast injection. *D*, CBF. *E*, CBV. *F*, MTT.

With regard to image quality, previous studies have shown that the physical performance (image noise, spatial resolution, contrast detectability, etc) and clinical image quality of 256-detector row CT are closely similar to those of MDCT (4, 8). The relatively low resolution of the present perfusion images is because the pig heads studied were smaller than the human head and because the commercial deconvolution algorithm used is smoother than other algorithms in reducing image noise. Nevertheless, this perfusion algorithm is used commercially in Toshiba CT scanners and has sufficient image quality for diagnosis. Because the volumetric perfusion analysis used deconvolution analysis to simply extend the conventional 2D analysis to a 3D analysis, the accuracy of the perfusion CT map in this study was closely similar to that in MDCT.

One limitation of volumetric perfusion CT is the high patient dose required. Although consideration must be given to dose minimization (9), high doses are presently unavoidable because the beam width of the 256-detector row CT is >3 times that of 64-detector row CT and because radiation scatter increases as beam width widens. Because volumetric perfusion CT imaging results vary widely depending on differences in patient blood circulation (10), minimization of imaging time requires appropriate timing of the scan after the start of contrast injection. As a result of its tremendous reduction in examination time, volumetric perfusion CT can be

used in critically ill or uncooperative patients without sedation or intubation. For commercial CT scanners, scanning conditions for cerebral perfusion are generally considered to be approximately 200 mAs and 30–50-second scan time (repeatable scans and intervals), giving total scan times of <25 seconds. In the present study, scan time was set at 50 seconds continuously, because the 256-detector row CT could not perform repeat scans and intervals. Wintermark et al (11) reported that 80-kV increased enhancement, gave better contrast between white and gray material, and lowered the patient dose by a factor of 2.8 compared with 120 kV. The effective dose was reduced by scanning with the gantry tilted to avoid the crystalline lens. When these dose-reduction methods were adopted to the 256-detector row CT, patient dose was reduced to <20 mSv. Although it is presently difficult to reduce patient dose with cone-beam CT to less than that for MDCT, we are now investigating dose reduction methods for volumetric perfusion CT.

In conclusion, the 256-detector row CT is a potentially easily available imaging technique that provides simultaneous cine imaging, CTA and perfusion CT with wide craniocaudal coverage, and in multiple planes. We are now developing a second 256-detector row CT model with a rotation time of .5 seconds and will report the use of this equipment in volumetric perfusion CT in humans.

References

1. Miles KA, Griffiths MR. **Perfusion CT: a worthwhile enhancement?** *Br J Radiol* 2003;76:220–231
2. Endo M, Mori S, Tsunoo T, et al. **Development and performance evaluation of the first model of 4DCT-scanner.** *IEEE Trans Nucl Sci* 2003;50:1667–1671
3. Mori S, Kondo C, Suzuki N, et al. **Volumetric cine imaging for cardiovascular circulation using prototype 256-detector row computed tomography scanner (4-dimensional computed tomography): a preliminary study with a porcine model.** *J Comput Assist Tomog* 2005;29:26–30
4. Mori S, Endo M, S, Tsunoo T, et al. **Physical performance evaluation of a 256-slice CT-scanner for 4-dimensional imaging.** *Med Phys* 2004;31:1348–1356
5. Saito Y, Aradate H, Igarashi K, et al. **Large area 2-dimensional detector for real-time 3-dimensional CT (4DCT).** *Proc SPIE* 2001;4320:775–782
6. Feldkamp LA, Davis LC, and Kress JW. **Practical cone-beam algorithm.** *J Opt Soc Am* 1984;A1:612–61
7. Meier P, Zierler KL. **On the theory of the indicator-dilution method for measurement of blood flow and volume.** *J Appl Physiol* 1954;6:731–744
8. Mori S, Endo M, Obata T, et al. **Clinical potentials of the prototype 256-detector row CT-scanner.** *Acad Radiol* 2005;22:149–155
9. Hsieh J, Wei Y, Wang G. **Fractional scan algorithms for low-dose perfusion CT.** *Med Phys* 2004;31:1251–1257
10. Silverman PM, Roberts SC, Ducic I, et al. **Assessment of a technology that permits individualized scan delays on helical hepatic CT: a technique to improve efficiency in use of contrast material.** *AJR Am J Roentgenol* 1996;167:79–84
11. Wintermark M, Maeder P, Verdun FR, et al. **Using 80 kVp versus 120 kVp in perfusion CT measurement of regional cerebral blood flow.** *AJNR Am J Neuroradiol* 1991;12:201–213